

## Induced ferroelectricity in strained epitaxial SrTiO<sub>3</sub> films on various substrates

R. Wördenweber, E. Hollmann, R. Kutzner, and J. Schubert

Citation: *Journal of Applied Physics* **102**, 044119 (2007);

View online: <https://doi.org/10.1063/1.2773680>

View Table of Contents: <http://aip.scitation.org/toc/jap/102/4>

Published by the *American Institute of Physics*

---

### Articles you may be interested in

[Ferroelectric thin films: Review of materials, properties, and applications](#)

*Journal of Applied Physics* **100**, 051606 (2006); 10.1063/1.2336999

[Relaxor ferroelectricity in strained epitaxial SrTiO<sub>3</sub> thin films on DyScO<sub>3</sub> substrates](#)

*Applied Physics Letters* **88**, 192907 (2006); 10.1063/1.2198088

[Impact of compressive in-plane strain on the ferroelectric properties of epitaxial NaNbO<sub>3</sub> films on \(110\) NdGaO<sub>3</sub>](#)

*Applied Physics Letters* **103**, 132908 (2013); 10.1063/1.4822328

[Effect of stoichiometry on the dielectric properties and soft mode behavior of strained epitaxial SrTiO<sub>3</sub> thin films on DyScO<sub>3</sub> substrates](#)

*Applied Physics Letters* **102**, 082905 (2013); 10.1063/1.4793649

[Influence of the oxidation state of SrTiO<sub>3</sub> plasmas for stoichiometric growth of pulsed laser deposition films identified by laser induced fluorescence](#)

*APL Materials* **3**, 106103 (2015); 10.1063/1.4933217

[Relaxor ferro- and paraelectricity in anisotropically strained SrTiO<sub>3</sub> films](#)

*Journal of Applied Physics* **113**, 164103 (2013); 10.1063/1.4802676

---



# SciLight

Sharp, quick summaries illuminating  
the latest physics research

Sign up for **FREE!**

AIP  
Publishing

# Induced ferroelectricity in strained epitaxial SrTiO<sub>3</sub> films on various substrates

R. Wördenweber,<sup>a)</sup> E. Hollmann, R. Kutzner, and J. Schubert

*Institut für Schichten und Grenzflächen (ISG) und CNI - Center of Nanoelectronic Systems for Information Technology, Forschungszentrum Jülich, D-52425 Jülich, Germany*

(Received 3 May 2007; accepted 10 July 2007; published online 30 August 2007)

The impact of strain on structure and ferroelectric properties of epitaxial SrTiO<sub>3</sub> films on various substrate materials—substrates with larger (DyScO<sub>3</sub>) and smaller (NdGaO<sub>3</sub> and CeO<sub>2</sub>/Al<sub>2</sub>O<sub>3</sub>) in-plane lattice constant, respectively—was analyzed. In all cases, (001)-oriented strained epitaxial SrTiO<sub>3</sub> was obtained. It is demonstrated that the mismatch of the lattices or, alternatively, the mismatch of the thermal expansion coefficients of films and substrate, imposes biaxial strain on the SrTiO<sub>3</sub> films. The strain leads to a small tetragonal distortion of the SrTiO<sub>3</sub> lattice and has a large impact on the ferroelectric properties of the films. With decreasing film thickness and at low temperatures the permittivity deviates from the “classical” Curie-Weiss behavior. Furthermore, strain-induced ferroelectricity is observed, which agrees with theoretical predictions. For electric fields parallel to the film, surface-induced ferroelectricity is observed for SrTiO<sub>3</sub> that is exposed to in-plane tensile strain, i.e., SrTiO<sub>3</sub> on DyScO<sub>3</sub> and sapphire. Transition temperatures of  $T_o \approx 210$  K and  $T_o \approx 325$  K are obtained for SrTiO<sub>3</sub> on CeO<sub>2</sub>/Al<sub>2</sub>O<sub>3</sub> and DyScO<sub>3</sub>, respectively.

© 2007 American Institute of Physics. [DOI: [10.1063/1.2773680](https://doi.org/10.1063/1.2773680)]

## I. INTRODUCTION

In the past, SrTiO<sub>3</sub> (STO) has been of considerable interest due to its low-temperature properties. Nowadays the interest has revived due to recently introduced concepts that allow modification or even engineering of the properties toward various electronic room-temperature applications in ferro- or paraelectric devices (e.g., spin-based electronics, tunable varactors, or phase shifters for microwave applications).

Generally, the dielectric properties of STO are qualitatively similar to those of the paraelectric phase of typical perovskite ferroelectrics like BaTiO<sub>3</sub>. In these materials a soft transverse optical mode exists whose frequency tends to zero with decreasing temperature.<sup>1,2</sup> This leads to an increase of the permittivity of STO when the material is cooled.<sup>3</sup> However, in contrast to BaTiO<sub>3</sub>, STO is an incipient ferroelectric or a quantum paraelectric,<sup>3–5</sup> i.e., it does not undergo a ferroelectric transition. This is attributed to quantum fluctuations in the material at low temperatures that suppress the ferroelectric transition. However, this quantum paraelectric state is very sensitive to perturbations of the lattice. Thus, a ferroelectric transition can be induced in STO by small levels of impurities or doping,<sup>6</sup> applied electric fields,<sup>7</sup> <sup>18</sup>O substitution,<sup>8</sup> or mechanical stress.<sup>9,10</sup> As a result the Curie temperature can be increased and the material can be made suitable for room-temperature applications. On the other hand, oxide ceramics have a large potential to serve as substrate material for the epitaxial growth of oxide ferroelectric thin films like STO. Depending on the composition of the substrate, different lattice constants and thermal expansions can be realized that result in different strain situations within the epitaxial film. This has recently been demonstrated for

STO on various substrates.<sup>11–13</sup> The “engineering” of the strain allows tuning of the ferroelectric properties or even induces ferroelectricity in the case of epitaxial STO films.

In this article the impact of strain on the structural and ferroelectric properties of epitaxial STO films grown on different substrate systems is analyzed. The strain is induced by mismatch of the lattice constant or thermal expansion coefficient, respectively. The permittivity is strongly affected by the strain and, depending on the amount and type of lattice distortion, ferroelectricity is induced in the STO layers up to elevated temperatures.

## II. EXPERIMENTAL RESULTS AND DISCUSSION

A series of STO films is grown on NdGaO<sub>3</sub> (110) (NGO), DyScO<sub>3</sub> (110) (DSO), and CeO<sub>2</sub> buffered r-cut sapphire (Al<sub>2</sub>O<sub>3</sub>) via pulsed laser deposition. In order to provide similar growth conditions, all STO layers are deposited at identical conditions. That is, the heater temperature is 850 °C, the process gas consists of pure O<sub>2</sub> at a pressure of 1 Pa, the laser power is about 5 J/cm<sup>2</sup> at the target, and 10 Hz repetition rate was chosen, resulting in a growth rate of 180 nm/min. The thicknesses of the STO layers are 185 and 105 nm for the films on NdGaO<sub>3</sub> and DyScO<sub>3</sub>, respectively. In the case of the films on CeO<sub>2</sub> [40 nm thickness and (001) oriented] buffered r-cut sapphire, a series of films with thicknesses ranging from 8 to 710 nm is prepared.

Due to the lattice mismatch, STO films on (110) DSO substrates are expected to be exposed to tensile strain, whereas (110) NGO or (001) CeO<sub>2</sub> would lead to compressive strain parallel to the film surface (in-plane). At room temperature, DSO and NGO adopt the orthorhombic (distorted) perovskite structure (GdFeO<sub>3</sub>-structure,  $P_{nma}$  space group 62).<sup>14</sup> The parameters  $a \neq b \neq c$  of the orthorhombic lattice (see Table I) are related to the pseudocubic lattice

<sup>a)</sup>Corresponding author; Electronic mail: [r.woerdenweber@fz-juelich.de](mailto:r.woerdenweber@fz-juelich.de)

TABLE I. Bulk lattice parameters of undistorted DyScO<sub>3</sub> (orthorhombic), NdGaO<sub>3</sub> (orthorhombic), CeO<sub>2</sub> (cubic), and SrTiO<sub>3</sub> (cubic). Furthermore, the effective lattice constant  $a_p$  for the epitaxial growth (e.g., pseudocubic lattice constant), theoretical lattice mismatch (between substrate and STO), the resulting expected tetragonality, and the thermal expansion coefficient (Ref. 19) are given for the chosen orientation of the substrate material.

	$a$ (nm)	$b$ (nm)	$c$ (nm)	Orientation	$a_p$ (nm)	Mismatch	Tetragonality	Thermal exp. coeff. [10 <sup>-6</sup> K <sup>-1</sup> ]
DyScO <sub>3</sub>	0.5449	0.7931	0.5726	(110)	0.395	+1.18%	0.9654	8.4
NdGaO <sub>3</sub>	0.543	0.772	0.550	(110)	0.386	-1.13%	1.0347	10.2
CeO <sub>2</sub> (cubic)		0.5411		(001)	0.3826	-2.00%	1.0625	
SrTiO <sub>3</sub> (cubic)		0.3904		(001)				9.4
Al <sub>2</sub> O <sub>3</sub>				r-cut	0.349	-10.8%		6-8.7

constant  $a_p$  of the cubic perovskites according to  $a \approx c \approx a_p\sqrt{2}$  and  $b = 2a_p$ , with  $a_p \approx 0.395$  nm and  $a_p \approx 0.386$  nm for (110) DSO and (110) NGO, respectively. In contrast, CeO<sub>2</sub> possesses a cubic fluorite-type structure with lattice constant  $a = b = c = 0.5411$  nm.<sup>14</sup> The cubic (001) STO grows in the [110] direction of the (001) CeO<sub>2</sub> on the resulting cubic lattice constant  $a \approx a_p\sqrt{2}$  with  $a_p \approx 0.3826$  nm. Therefore, the resulting lattice mismatch between these substrates and STO film is expected to be +1.18% for DSO, -1.13% for NGO, and -2.00% for CeO<sub>2</sub>, respectively.

The crystalline properties of the different layers are analyzed via high-resolution x-ray diffraction (XRD). The measurements yield, among others, the epitaxial orientation, structural quality, lattice parameters, and mutual angular orientation of the different layers. It should be noted that the XRD data represent integral properties of the film structure at room temperature. The impact of the thermal expansion of the film's structure over the thickness of the films cannot be recorded with this analysis.

The XRD results can be summarized in the following way. All STO films grow epitaxially. No STO phases other than [001] orientation are detected. The STO lattice parameters are obtained from the XRD measurements in Bragg-Brentano geometry using the Nelson-Riley correction of (00 $\ell$ ) peaks. The resulting lattice parameters (normal and parallel to the film surface) of the STO layers are shown in Fig. 1. For comparison, literature values for the lattice parameters of (undistorted) STO, CeO<sub>2</sub>, NGO, and DSO are added.<sup>14</sup>

The STO films on NGO and DSO behave as expected. The in-plane lattice parameter  $a_{\parallel}$  is elongated or distorted for STO on DSO or on NGO, respectively. This modification of the lattice parameter perfectly agrees with the expected impact of the lattice parameter of the underlying substrate [see Fig. 1(b)]. As a consequence the out-of-plane lattice parameter  $a_{\perp}$  is also modified. However, this modification occurs in the opposite way in order to (partially) compensate the effect of the in-plane strain upon the volume of the unit cell, i.e.,  $a_{\perp}$  is elongated for NGO and reduced for DSO. The resulting measured volume of the unit cell slightly deviates from the literature value by  $\pm 1.7\%$  (depending on the substrate) and the tetragonality is smaller than expected, i.e.,  $a_{\parallel}/a_{\perp} = 0.987$  and 1.016 for NGO and DSO, respectively (compare with Table I).

The STO films on CeO<sub>2</sub> buffered sapphire behave quite differently. For all films (8 to 710 nm) both lattice parameters (normal and perpendicular to the surface) are quite similar to the literature value of undistorted STO. Thus, our STO films on CeO<sub>2</sub>/sapphire seem to be nearly unstrained at room temperature. The lattice mismatch between the CeO<sub>2</sub> and STO does not seem to affect the in-plane lattice parameter of the STO in the same way as is observed for the other systems (STO on NGO and DSO). There are different possible explanations for this distinct difference. Considering also the discussion of the ferroelectric properties of these films (see below), we would favor the following interpretation.

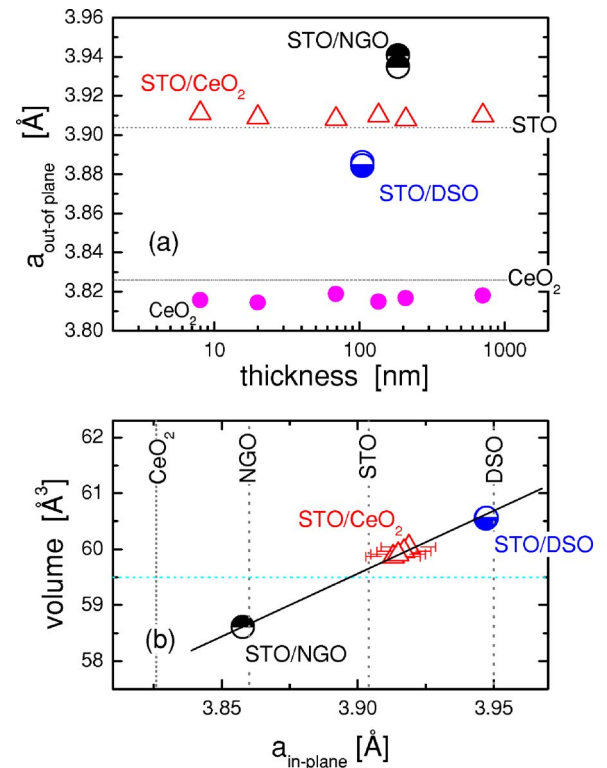


FIG. 1. STO lattice parameters normal and parallel to the substrate surface. In (a) the thickness dependence of the out-of-plane lattice parameter  $a_{\perp}$  of STO and, for the films on sapphire,  $a_p$  of CeO<sub>2</sub> are given. In (b) the volume of the unit cell is plotted as function of the in-plane lattice parameter  $a_{\parallel}$ . The latter is obtained from XRD measurements of (111) and (103) reflexes. For undistorted STO a volume of the unit cell of 59.5 Å<sup>3</sup> is expected (see dotted line). Literature values for the undistorted lattice parameters (or  $a_p$ ) of the different systems are added in both plots.

First, in the case of DSO and NGO, STO grows on a (pseudo-) cubic lattice with an only slightly larger (DSO) or smaller (NGO) lattice constant  $a_p$  (see Table I). In contrast, on  $\text{CeO}_2$  (a) the effective lattice mismatch is much larger and (b) the STO grows under a  $45^\circ$  in-plane rotation with only half of the Sr positions matched to a Ce atomic position. This is a quite different type of epitaxy. In this way, distortions and defects can easily be accommodated at the STO/ $\text{CeO}_2$  interface and can lead to a growth with strongly reduced lattice-induced strain.

Second, additional to the lattice mismatch, differences in the thermal expansion between substrate and STO film do lead to strain in the film. This effect depends on the expansion coefficient and is obviously temperature dependent. It seems to be small for NGO and DSO. Furthermore, for these substrates this effect does not counteract the effect of lattice mismatch (see Table I). However, for STO grown on sapphire the difference in thermal expansion coefficient seems to be important. The film is grown at elevated temperature ( $850^\circ\text{C}$ ). Upon cooling, the substrate shrinks less than the STO film, which results in a compensation of the strain at given temperature and, subsequently, even a tensile in-plane strain at lower temperatures. This might be the explanation for the slight tensile in-plane strain observed for some of our STO films on sapphire [see Fig. 1(b)] that is in contrast to the expected compressive in-plane strain due to lattice mismatch. This might also be the reason for the induced ferroelectricity at relatively high temperatures in this system that is demonstrated and discussed below.

The dielectric properties of the STO films are determined by capacitance measurements of planar capacitors at 1 MHz and 2–4 GHz. These experiments selectively record the in-plane polarization with an accuracy better than 1%. Furthermore, a comparison of the low-frequency data and measurements up to the terahertz regime<sup>15</sup> demonstrates that the permittivity is independent of frequency up to about 0.5 THz for our samples. Figure 2 shows a comparison of the temperature and thickness dependence of the permittivity (at zero bias voltage and electric field component parallel to the surface) for the STO films on sapphire and, for comparison, a STO single crystal.

First, the room-temperature permittivity measured for thick STO films ( $h_f > 100$  nm) is similar to that of the single crystal [i.e.,  $\epsilon(300\text{ K}) \approx 350$ ], whereas, for thin STO films ( $h_f < 100$  nm) the permittivity increases with decreasing thickness. For our thinnest sample ( $h_f = 8$  nm) we measured  $\epsilon(300\text{ K}) \approx 790$ , which is more than twice as large compared to the value obtained for single crystals.

Second, the STO single crystal and the thicker STO films ( $h_f > 100$  nm) show perfect Curie-Weiss behavior for elevated temperatures, i.e.,  $\epsilon = C/(T - T_c)$ . The resulting Curie-Weiss temperature  $T_c \approx 40$  K is comparable to the literature values for bulk STO. Moreover, even a quantitative agreement of the  $\epsilon(T)$ -values of single crystals and thick films is given for high temperatures. Only for  $T < 150$  K the data diverge. With decreasing temperature the permittivity of the single crystal outranges the permittivity of the thick films by far.

Finally, with decreasing thickness of the STO layers

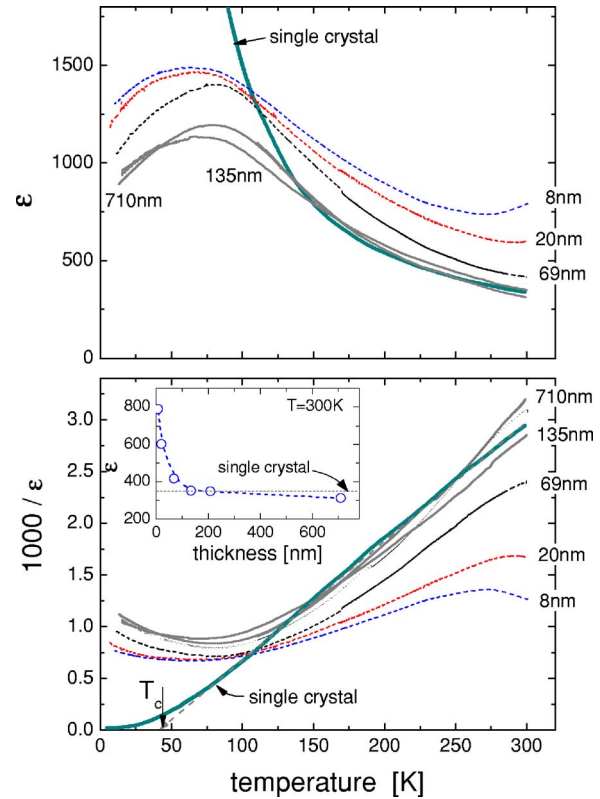


FIG. 2. Temperature dependence of the permittivity (a) and inverse permittivity (b) for STO films on  $\text{CeO}_2$  buffered sapphire (the numbers represent the thickness of the STO films) and a STO single crystal. The inset shows the thickness dependence of the permittivity of the STO films (circles) and the permittivity of the single crystal measured at room temperature.

( $h_f < 100$  nm), the high-temperature behavior of the permittivity diverges more and more from the Curie-Weiss behavior of the single-crystalline STO. Whereas the film with a thickness of  $h_f = 69$  nm still shows Curie-Weiss behavior with a  $T_c$  comparable to that of bulk material (but with enhanced permittivity), the temperature dependence of  $\epsilon^{-1}$  of the thinnest films ( $h_f < 25$  nm) is not Curie-Weiss-type. Furthermore, the curves obtained for the thinner samples show a clear maximum around room temperature. The position of this maximum shifts to lower temperatures with decreasing film thickness.

The thickness dependence of the room-temperature permittivity and the different temperature dependences of  $\epsilon^{-1}$  (Fig. 2) can consistently be explained by the scenario that has been sketched above for the explanation of the structural data:

- The strain is relaxed over the STO film thickness. This explains the quantitative and qualitative (Curie-Weiss behavior) agreement of the permittivity of thick films ( $h_f > 100$  nm) and single crystals at elevated temperatures ( $T > 150$  K).
- In thinner STO films ( $h_f < 100$  nm) the strain cannot relax or only partially relax, which results in a modification (increase) of the permittivity at room temperature.
- The deviation from the Curie-Weiss behavior and, especially, the maximum in the temperature dependence



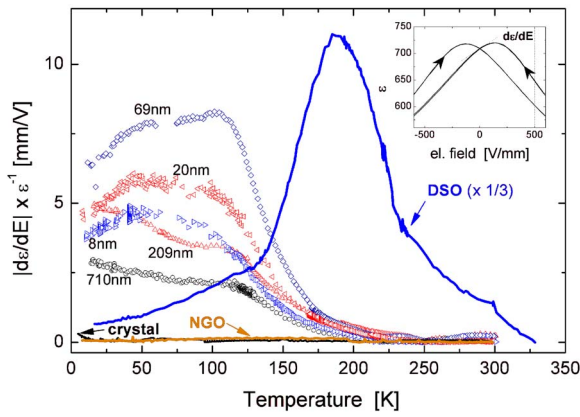


FIG. 3. Temperature dependence of the normalized slope  $|d\epsilon/dE| \times \epsilon^{-1}$  at zero voltage obtained after application of large positive or negative bias fields, respectively, for STO films on different substrates and a STO single crystal. The data of STO on DSO are reduced by a factor of 3. The electric fields are applied parallel to the film surface.

of  $\epsilon^{-1}$  observed for thin films, indicates that the strain in this system (STO on  $\text{CeO}_2/\text{Al}_2\text{O}_3$ ) is not dominated by the lattice mismatch between carrier and STO. It is more likely that the difference in thermal expansion between the substrate and the STO film leads to a temperature-dependent strain in the films on sapphire. This is consistent with the XRD observations that are discussed above. It can also explain the deviation from Curie-Weiss behavior that is observed for all films (even the thick STO layers) at low temperatures (Fig. 2).

In contrast to the single crystal, some thin films show a large paraelectric tunability and ferroelectricity up to elevated temperatures. A hysteretic behavior of the current-voltage characteristics is a clear fingerprint of the presence of ferroelectricity (inset, Fig. 3). Thus, the presence of ferroelectricity can be analyzed by measurements of the slope  $d\epsilon/dE$  at zero voltage which is obtained after applying a large positive or negative bias field  $E$ , respectively. For hysteretic behavior (i.e., ferroelectricity) a nonzero value of  $d\epsilon/dE$  should be measured. In order to distinguish between real ferroelectricity and relaxor behavior,<sup>11</sup> the measurement was performed at different frequencies (kHz-GHz) and amplitudes of the detection field.

Figure 3 shows the temperature dependence of the normalized slope  $|d\epsilon/dE|/\epsilon$  for zero-bias field for our films and, for comparison, an unstrained STO single crystal. In our planar capacitor structures (gap of 4  $\mu\text{m}$ ), the electric bias field is applied parallel to the film surface. The STO single crystal and the STO film on NGO show no indication of ferroelectricity down to the lowest temperature of 4 K (i.e.,  $|d\epsilon/dE|/\epsilon \approx 0$ ), whereas the films on DSO and sapphire show nonzero values up to elevated temperatures. According to these measurements, ferroelectricity is present in STO on  $\text{CeO}_2/\text{Al}_2\text{O}_3$  up to about  $T_o \approx 200$ –220 K, although the Curie temperature  $T_c \approx 40$  K is not changed. The temperature dependence of  $|d\epsilon/dE|/\epsilon$  is similar and the transition temperature  $T_o$  is independent of the thickness of the films on sapphire. For STO on DSO ferroelectricity persists even up to room temperature, i.e.,  $T_o \approx 325$  K.

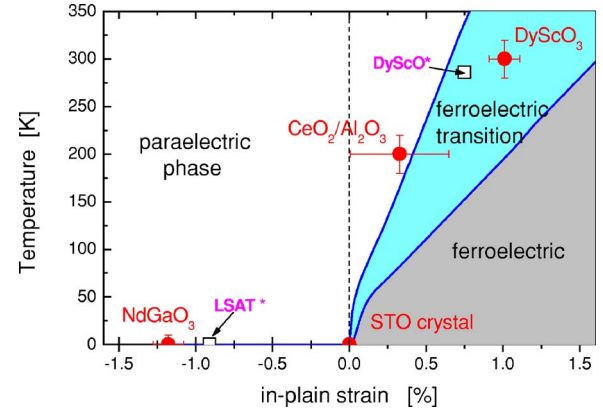


FIG. 4. Shift of the transition temperature  $T_o$  of (001) STO as function of the biaxial in-plane strain for electric fields (bias and rf field) parallel to the film surface. Theoretical predictions (Ref. 16) and literature values for STO on DSO and LSAT (Ref. 18) are added.

The temperatures of phase transition can be compared with theoretical predictions for induced ferroelectricity due to biaxial strain in epitaxial STO thin films.<sup>16,17</sup> These predictions are based on the Landau-Ginsburg-Devonshire theory and minimization of the Helmholtz free energy, taking into account the electric polarization in a bias field. It predicts true ferroelectric phases due to the coupling between the polarization and strain (electrostriction), the resulting transition temperatures for STO films are calculated as function of strain (see Fig. 4). For our configuration ( $E$  parallel to the film surface) an enhancement of  $T_o$  is predicted for tensile strain only. Our data (and literature data<sup>18</sup>) confirm this tendency (Fig. 4). No phase transition ( $T_o < 4$  K) is measured for STO on NGO and the single crystal, whereas  $T_o \gg 4$  K for STO on DSO and  $\text{CeO}_2/\text{Al}_2\text{O}_3$  are obtained. Moreover, even the quantitative agreement is excellent. Taking into account, that the strain (given by the lattice mismatch measured at room temperature) for STO on  $\text{CeO}_2/\text{Al}_2\text{O}_3$  is probably underestimated at  $T_o \approx 210$  K, even the data for STO on  $\text{CeO}_2/\text{Al}_2\text{O}_3$  might perfectly fit to the theoretical prediction.

### III. CONCLUSIONS

The impact of strain on structure and ferroelectric properties of epitaxial  $\text{SrTiO}_3$  films is analyzed. STO films are grown on substrates with larger (DSO) and smaller (NGO and  $\text{CeO}_2/\text{Al}_2\text{O}_3$ ) in-plane lattice constant  $a_p$ . In all cases (001)-oriented strained epitaxial STO is obtained. In the case of films that are directly grown onto the single-crystalline carrier (DSO and NGO), the strain is dominated by the lattice mismatch between substrate and film, whereas for STO on  $\text{CeO}_2$  the difference in thermal expansion for substrate and film seems to be responsible for the strain. In the latter case, the STO films are exposed to tensile in-plane strain in spite of the negative lattice mismatch. Possible explanations are given for the different epitaxial growth mechanisms that are observed for these systems. The in-plane strain leads to a modification of the in-plane lattice constant. As a result, the out-of plane lattice constant is also modified in order to con-

serve the volume of the unit cell. However, this conservation of the volume of the unit cell is incomplete; the tetragonality is smaller than theoretically expected.

Furthermore, the impact of strain on the ferroelectric properties is demonstrated for the different systems. With decreasing film thickness and at low temperatures the permittivity deviates from the classical Curie-Weiss behavior for STO on sapphire. In comparison to the single crystal, a more than twice as large permittivity is measured at room temperature for the thinnest sample (8 nm). The deviation from the Curie-Weiss behavior and the thickness dependence of the permittivity can be explained by the same scenario that is used for the explanation of the structural data.

Finally, strain-induced ferroelectricity is observed for two of the systems. These observations agree with theoretical predictions based on the Landau-Ginsburg-Devonshire theory.<sup>16,17</sup> For electric fields parallel to the film, surface-induced ferroelectricity is present in STO films that are exposed to in-plane tensile strain, i.e., STO on DSO and sapphire. Transition temperatures of  $T_o \approx 210$  K and  $T_o \approx 325$  K are obtained for STO on  $\text{CeO}_2/\text{Al}_2\text{O}_3$  and DSO, respectively. Due to the orientation of the electric field, no ferroelectricity is recorded for STO on NGO, i.e., compressive in-plane strain is expected to lead to modification of the polarization normal to the film surface.<sup>13,16,17</sup>

In general, our experiments demonstrate that mismatch of the lattices or mismatch of the thermal expansion coefficients of films and substrate imposes biaxial strain on STO films. Since the strain leads to modification of the structural and ferroelectric properties of STO, the use of different substrate materials might be of interest for engineering the ferroelectric properties of these materials. This could lead to the development of improved electronic applications in the field of spintronic, tunable microwave devices, or even electrocalorimetric devices.

## ACKNOWLEDGMENTS

The authors would like to thank G. Pickartz, H. P. Böchem, M. Nonn, N. Klein, and A. Offenhäuser for their valuable support.

- <sup>1</sup>P. A. Fleury and J. M. Worlock, Phys. Rev. **174**, 613 (1968).
- <sup>2</sup>H. Vogt, Phys. Rev. B **51**, 8046 (1995).
- <sup>3</sup>K. A. Müller and R. Burkard, Phys. Rev. B **19**, 3593 (1979).
- <sup>4</sup>O. E. Kvyatkovskii, Solid State Commun. **117**, 455 (2001).
- <sup>5</sup>W. Zhong and D. Vanderbilt, Phys. Rev. B **53**, 5047 (1996).
- <sup>6</sup>J. G. Bednorz and K. A. Müller, Phys. Rev. Lett. **52**, 2289 (1984); W. Kleemann, J. Dec, Y. G. Wang, P. Lehnen, and S. A. Prosandeev, J. Phys. Chem. Solids **61**, 167 (2000); C. Ang, Z. Yu, P. M. Vilarinho, and J. L. Baptista, Phys. Rev. B **57**, 7403 (1998); W. Kleemann, A. Albertini, M. Kuss, and R. Lindner, Ferroelectrics **203**, 57 (1997); W. Kleemann, J. Dec, Y. G. Wang, P. Lehnen, and S. A. Prosandeev, J. Phys. Chem. Solids **61**, 167 (2000); G. A. Samara, J. Phys.: Condens. Matter **15**, R367 (2003); B. E. Vugmeister and M. D. Glinchuk, Rev. Mod. Phys. **62**, 993 (1990); C. Ang and Z. Yu, J. Appl. Phys. **91**, 1487 (2002); C. Ang, Z. Yu, and Z. Jing, Phys. Rev. B **61**, 957 (2000).
- <sup>7</sup>E. Hegenbarth, Phys. Status Solidi **6**, 333 (1964); P. A. Fleury and J. M. Worlock, Phys. Rev. **174**, 613 (1968); J. Hemberger, P. Lunkenheimer, R. Viana, R. Bohmer, and A. Loidl, Phys. Rev. B **52**, 13159 (1995); D. Fuchs, C. W. Schneider, R. Schneider, and H. Rietschel, J. Appl. Phys. **85**, 7362 (1999).
- <sup>8</sup>M. Itoh, R. Wang, Y. Inaguma, T. Yamaguchi, Y.-J. Shan, and T. Nakamura, Phys. Rev. Lett. **82**, 3540 (1999).
- <sup>9</sup>H. Uwe and T. Sakudo, Phys. Rev. B **13**, 271 (1976).
- <sup>10</sup>H.-C. Li, W. Si, R.-L. Wang, Y. Xuan, B. T. Liu, and X. X. Xi, Mater. Sci. Eng. B **56**, 218 (1998).
- <sup>11</sup>M. D. Biegalski, Y. Jia, D. G. Schlom, S. Trolier-McKinstry, S. K. Streiffer, V. Sherman, R. Uecker, and P. Reiche, Appl. Phys. Lett. **88**, 192907 (2006).
- <sup>12</sup>T. Yamada, J. Petzelt, A. K. Tagantsev, S. Denisov, D. Noujni, P. K. Petrov, A. Mackova, K. Fujito, T. Kiguchi, K. Shinozaki, N. Mizutani, V. O. Sherman, P. Muralt, and N. Setter, Phys. Rev. Lett. **96**, 157602 (2006).
- <sup>13</sup>T. Ostapchuk, J. Petzelt, V. Zelezny, A. Pashkin, J. Pokorny, I. Drbohlav, R. Kuzel, D. Rafaja, B. P. Gorshunov, M. Dressel, Ch. Ohly, S. Hoffmann-Eifert, and R. Waser, Phys. Rev. B **66**, 235406 (2002); D. Rafaja, J. Kub, D. Šimek, J. Lindner, and J. Petzelt, Thin Solid Films **422**, 8 (2002).
- <sup>14</sup>International Centre for Diffraction Data, Powder Diffraction File Database, Sets 1–45, Data Nos. 07–204, 21–972, 34–394.
- <sup>15</sup>P. Kuzel, F. Kadlec, H. Nemeč, R. Ott, E. Hoffmann, and N. Klein, Appl. Phys. Lett. **88**, 102901 (2006).
- <sup>16</sup>N. A. Pertsev, A. K. Tagantsev, N. Setter, Phys. Rev. B **61**, R825 (2000); Phys. Rev. B **65**, 219901 (2002).
- <sup>17</sup>Y. L. Li, S. Choudhury, J. H. Haeni, M. D. Biegalski, A. Vasudevarao, A. Sharan, H. Z. Ma, J. Levy, V. Gopalan, S. Trolier-McKinstry, D. G. Schlom, Q. X. Jia, and L. Q. Chen, Phys. Rev. B **73**, 184112 (2006).
- <sup>18</sup>J. H. Haeni, P. Irvin, W. Chang, R. Uecker, P. Reiche, Y. L. Li, S. Choudhury, W. Tian, M. E. Hawley, B. Craigo, A. K. Tagantsev, X. Q. Pan, S. K. Streiffer, L. Q. Chen, S. W. Kirchoefer, J. Levy, and D. G. Schlom, Nature **430**, 758 (2004).
- <sup>19</sup>T. R. Taylor, P. J. Hansen, B. Acikel, N. Pervéz, R. A. York, S. K. Streiffer, and J. S. Speck, Appl. Phys. Lett. **80**, 1978 (2002).